Published in final edited form as:
Biochemistry. 2013 December 17; 52(50): 8975–8983. doi:10.1021/bi4013534.

Mechanism of Enhanced Superoxide Production in the Cytochrome b_6f Complex of Oxygenic Photosynthesis

Danas Baniulis[1,2,*], **S. Saif Hasan**[1,*], **Jason T. Stofleth**[1,3], and **William A. Cramer**[1,¶]

[1]Department of Biological Sciences, Hockmeyer Hall of Structural Biology, Purdue University, West Lafayette, IN 47907, USA

Abstract

The specific rate of superoxide ($O_2^{\cdot-}$) production in purified active crystallizable cytochrome b_6f complex, normalized to the rate of electron transport, has been found to be an order of magnitude greater than that measured in isolated yeast respiratory bc_1 complex. The biochemical and structural basis for the enhanced production of $O_2^{\cdot-}$ in the cytochrome b_6f compared to the bc_1 complex is discussed. The larger rate of superoxide production in the b_6f complex could be a consequence of an increased residence time of plastosemiquinone/plastoquinol in its binding niche near the Rieske protein iron-sulfur cluster, resulting from (i) occlusion of the quinone portal by the phytyl chain of the unique bound chlorophyll, (ii) an altered environment of the proton-accepting glutamate believed to be a proton acceptor from semiquinone, or (iii) a more negative redox potential of the heme b_p on the electrochemically positive side of the complex. The enhanced rate of superoxide production in the b_6f complex is physiologically significant as chloroplast-generated ROS functions in the regulation of excess excitation energy, is a source of oxidative damage inflicted during photosynthetic reactions, and is a major source of ROS in plant cells. Altered levels of ROS production are believed to convey redox signaling from the organelle to the cytosol and nucleus.

Keywords

cytochrome; plastosemiquinone; signaling; superoxide

Introduction

The protein subunits and prosthetic groups in the structure from the cyanobacterium, *M. laminosus* [(1)] are shown (Fig. 1). The role of the cytochrome bc_1 complex in $O_2^{\cdot-}$ generation

¶To whom correspondence and requests for distribution of materials should be addressed: William A. Cramer, Dept. of Biological Sciences, Hockmeyer Hall of Structural Biology, Purdue University, West Lafayette, IN 47907, USA; Tel. 765-494-4956; waclab@purdue.edu.
[2]present address: Institute of Horticulture, Lithuanian Research Centre for Agriculture and Forestry, Babtai, Kaunas reg. Lithuania, LT – 54333, Lithuania
[3]present address: Dept. of Chemistry and Biochemistry, University of California/San Diego 92037
*shared senior authorship

Author Contributions. DB designed superoxide experiments, purified cytochrome b_6f complex, performed enzymatic assays, analyzed results, contributed to manuscript; SSH applied results to critical aspects of crystal structure, wrote manuscript; JTS purified cytochrome b_6f complex, performed enzyme assays, contributed to analysis of results; WAC conceived original idea, designed experiments, analyzed results, wrote manuscript.

by the mitochondrial respiratory electron transport pathway has been described and reviewed [2-8]. By analogy with the bc_1 complex, the site of production of superoxide in the cytochrome b_6f complex is shown (Fig. 2), with an emphasis on the electrochemically positive (p, lumen)-side plastoquinone/ol binding site which, by analogy with the mechanism proposed for the bc_1 complex, is close to the site of oxygen reduction by plastosemiquinone and resulting superoxide formation. The production of reactive oxygen species (ROS) in chloroplasts not only underlies oxidative damage inflicted in photosynthetic electron transport [9], but also functions in redox signaling from the organelle to the cytosol and nucleus [10], and in the regulation and dissipation of excess excitation energy [11]. Although $O_2^{\cdot-}$ production by the cytochrome b_6f complex of oxygenic photosynthesis has been detected by EPR spectroscopy [12], details on rates and constraints have not yet been determined. The present studies provide quantitative information on the level of $O_2^{\cdot-}$ generated in electron transport through the b_6f complex that mediates these signaling processes.

$O_2^{\cdot-}$ can be formed through a one electron reduction of the oxygen molecule, with a midpoint redox potential -0.14 V in the aqueous phase [13, 14].

$$O_2 + e^- \rightarrow O_2^{\cdot-} \quad \text{(i)}$$

Ubisemiquinone, $UQ_p^{\cdot-}$, formed on the electrochemically positive, p-side, of the complex (reaction iia) is a reductant for oxygen proximal to the bc_1 complex in mitochondrial and photosynthetic bacterial membranes. Because ubisemiquinol is a reductant of the low potential heme b_p in the bc_1 complex [15], it has been inferred that the ubisemiquinone formed in the bc_1 complex through quinol oxidation by the high potential segment of the electron transport chain has a sufficiently reducing potential to form superoxide, $O_2^{\cdot-}$ (reaction iia). Based on the similarity of the crystal structures of the protein core [16], and of the midpoint redox potentials, E_{m7} = +80 mV (plastoquinone/quinol, [17] and +60 mV, ubiquinone/quinol [18]), it is inferred that plastosemiquinone, $PQ_p^{\cdot-}$ can serve as the reductant for generation of superoxide in the b_6f complex (Fig. 2B, reaction iib):

$$UQ_p^{\cdot-} + O_2 \rightarrow UQ(ox) + O_2^{\cdot-} \quad \text{(iia)}$$

$$PQ_p^{\cdot-} + O_2 \rightarrow PQ(ox) + O_2^{\cdot-} \quad \text{(iib)}$$

The p-side semiquinone, $Q_p^{\cdot-}$, is generated through the one electron oxidation of ubiquinol or plastoquinol, QH_2, by the iron-sulfur [FeS] cluster of the high potential Rieske iron-sulfur protein subunit of the complex:

$$QH_2 + [FeS](ox) \rightarrow QH_p^{\cdot} + [FeS](red) + H^+ \quad \text{(iii)}$$

$QH_p^{\cdot-}$ generated in reaction (iii) transfers a proton to the p-side aqueous phase through an intra-protein pathway in the cytochrome bc_1 complex [19]. A similar p-side proton release

pathway, which forms the p-side anionic plastosemiquinone, $PQ_p^{\cdot-}$, has recently been defined by crystallographic analysis of the cytochrome b_6f complex [20].

In a Q-cycle mechanism [15, 21-24], an electron is transferred from the deprotonated $Q_p^{\cdot-}$, to the p-side heme b_p (reaction iv), and then across the hydrophobic domain of the membrane through the n-side heme, b_n to reduce quinone specifically bound on the 'n' side of the complex.

$$Q_p^{\cdot-} + b_p(ox) \rightarrow b_p(red) + Q_p(ox) \quad \text{(iv)}$$

Reduced heme b_p may be an alternative source of electrons for the reduction of O_2 to $O_2^{\cdot-}$ [25]:

$$b_p(red) + O_2 \rightarrow b_p(ox) + O_2^{\cdot-} \quad \text{(v)}$$

It has been inferred [2, 8] that superoxide production in the cytochrome bc_1 complex occurs as a by-pass of step **iv** above of the Q-cycle by reactions iia, b or v, the latter reaction having been suggested as dominant [4, 25]. The participation of reactions iib and v in super-oxide generation in the cytochrome b_6f complex is shown in Q-cycle scheme (Fig. 2). The n-side ubiquinone reduction in the bc_1 complex is blocked by the quinone analogue inhibitor antimycin A, which occupies the n-side quinone binding site with high affinity [26]. A consequence of this inhibition of the trans-membrane electron transfer chain would be accumulation of the p-side semiquinone electron donor, $Q_p^{\cdot-}$ (reaction iv). The probability of electron transfer through the other branch of the $UQ_p^{\cdot-}$ oxidation pathway that forms superoxide (reaction iia) would then be increased. Thus, the specific n-side quinone analogue inhibitor, antimycin A, causes a large increase in the specific rate of formation of $O_2^{\cdot-}$, relative to the electron transport rate, by the bc_1 complex of yeast or bovine mitochondria [4, 7, 8, 27, 28], and the photosynthetic bacterium, *Rb. sphaeroides* [29]. No n-side inhibitor comparable in efficacy to that of antimycin. has been found for the b_6f complex, because the unique heme c_n occupies the quinone binding site homologous to that of antimycin [30], which results in an altered binding-interaction of an n-side quinone analogue inhibitor [31]. Although the quinone analogue inhibitor NQNO, binds specifically to the n-side heme c_n [1], and inhibits the oxidation of heme b_n [32-34], unlike the inhibition of the respiratory chain resulting from the action of antimycin, the extent of inhibition of linear electron transport, by NQNO, is small [32].

It has been proposed that $O_2^{\cdot-}$ production occurs in the cytochrome b_6f complex [2] by a mechanism (reaction iib) similar to the alternative pathway for the bc_1 complex (reaction iia) [2, 3, 5, 8]. However, experimental details on the rate of $O_2^{\cdot-}$ generation in the b_6f complex have not been described. The present study compares the specific rate of $O_2^{\cdot-}$ generation in cytochrome b_6f and bc_1 complexes, and proposes that the level of $O_2^{\cdot-}$ production by the b_6f and bc_1 complexes is dependent upon the residence time of reduced quinone species within the Q_p-portal.

Materials and Methods

Materials

ADPH and H_2O_2 were purchased from Anaspec (Fremont, CA), equine heart cytochrome *c*, HRP and SOD enzymes, decyl-ubiquinol and decyl-plastoquinol from Sigma-Aldrich (St. Louis, MO), and DDM/UDM from Anatrace (Maumee, OH), and other reagents from Mallinckrodt/Baker, Inc. (Phillipsburg, NJ).

Preparation of yeast mitochondrial cytochrome bc_1 complex

Cytochrome bc_1 complex from yeast was purified in the laboratory of B. L. Trumpower, as previously described [28].

Preparation of thylakoid membranes and purification of cytochrome b_6f complex

Cyanobacterial thylakoid membranes were prepared and b_6f complex purified as described [35], as were spinach chloroplast thylakoid membranes and cytochrome b_6f complex [35, 36]. Membranes were re-suspended (chlorophyll *a* concentration, 2 mg/ml) in TNE (30 mM Tris-HCl, pH 7.5, 50 mM NaCl, 1 mM EDTA, 0.3 M sucrose, with protease inhibitors, benzamidine (2 mM) and ε-amino-caproic acid (2 mM).

Purification of plastocyanin

Plastocyanin *from Nostoc* [36] and spinach [37] was purified as described and, for the latter, a modified procedure included size exclusion and anion-exchange chromatography.

Activities for ubiquinol-cytochrome c and plasto-quinol-plastocyanin, oxido-reductase were assayed, respectively, with purified bc_1 and b_6f complex. For the bc_1 complex, the assay mixture contained 50 μM equine heart cyt *c*, 50 mM MOPS, pH 6.9, 0.4 mM DDM, 1 mM KCN, and 0.05 mM decyl-ubiquinol. Reduction of cyt *c*, initiated by addition of 5 or 45 nM cytochrome bc_1 for uninhibited and inhibited activity, respectively, was monitored through the absorbance change at 551 nm and the activity was based on an extinction coefficient of $2.1 \times 10^{(4)}$ $M^{-1}cm^{-1}$ [38]. For the plastoquinol-plastocyanin oxido-reductase activity of b_6f complex or thylakoid membranes, the assay mixture contained plastocyanin (10^{-2} M) from *Nostoc* or spinach, 50 mM Tris-HCl, pH 7.5, 1 mM UDM, and 20 μM decyl-plastoquinol. Absorbance changes were assayed on a Cary 4000 spectrophotometer. The reaction was initiated by addition of 5 nM cyt b_6f complex or 3 μM Chl-*a* equivalent of thylakoid membranes, and activity monitored as the change of plastocyanin absorbance at 597 nm (ε_{mM} = 4.9 $mM^{-1}cm^{-1}$ [39]). Inhibitors were added as ethanol stocks (less than 0.5% of total reaction volume). Initial electron transport rates were determined using the SLOPE function in the support software of a Cary 4000 spectrophotometer, and calculated as moles electrons transferred per mol *bc* complex sec^{-1}, or per $10^{(3)}$ mol Chl-*a* equivalent of thylakoid membranes.

Superoxide production assay

Superoxide released from cytochrome *bc* complexes was measured fluorometrically via formation of H_2O_2. In the presence of saturating levels of SOD, superoxide released from cytochrome *bc* complexes is converted to H_2O_2. ADPH reacts with H_2O_2 in a 1:1

stoichiometry, in the presence of HRP as a catalyst, to produce the fluorescent oxidation product, resorufin. The reaction mixture contained: (**i**) for yeast bc_1 complex- 50 mM MOPS, pH 6.9, 0.4 mM DDM, 50 μM ADHP, 1 U/mL HRP, equine heart cyt *c* 50 μM, 50 μM decyl-ubiquinol; and for b_6f complex- 50 mM MOPS, pH 6.9, 1 mM UDM, 40 μM ADPH, 20 μM decyl-plastoquinol, 1 U/mL HRP, 300 U/ml SOD, plastocyanin (10 mM) from *Nostoc* or spinach, or 25 μM cyt *c* from equine heart. Inhibitors were added as ethanol stocks (less than 0.5% of total reaction volume). The reaction was started by adding bc_1 complex to a final concentration of 5 or 45 nM for measurement of uninhibited and inhibited activity, respectively, or b_6f complex to 5 nM (3 μM Chl-*a* equivalent of thylakoid membranes). The fluorescence indicator of superoxide production was measured by excitation and emission at 530 nm (2 nm band width) and 590 nm (1 nm band width) respectively, utilizing a FluoroMax-3 fluorimeter (Horiba Jobin Yvon Inc., Edison, NJ), and calibrated using H_2O_2 standards. The initial rate of superoxide production was estimated using the LINEST function of MS Office Excel software and calculated as moles superoxide generated·sec^{-1} mol^{-1} *bc* complex, or per $10^{(3)}$ mol Chl-*a* equivalent of thylakoid membranes.

Sequence alignment was performed with Clustal-Omega using default parameters [40, 41]. Cytochrome b_6 polypeptide sequences were obtained from the NCBI database, with accession numbers: *Synechocystis* sp. PCC 6803, BAA10149.1; *Synechococcus elongatus* PCC 6301, BAD79961.1; *Nostoc* sp. PCC 7120, BAB75120.1; *Mastigocladus laminosus*, AAR26242.1; *Chlamydomonas reinhardtii*, CAA44690.1; *Arabidopsis thaliana*, NP_051088.1; *Spinacea oleracea*, CAA30128.1.

Figure 4A, B was generated in Pymol (www.pymol.org), from structural superposition of cytochrome bc_1 complex crystal structures (PDB IDs 1NTZ [42] and 3CX5 [43]), and cytochrome b_6f complex crystal structures (PDB IDs 4H44 and 4H13 [20]).

Results

Superoxide production in the cytochrome bc_1 complex

The rate of superoxide ($O_2^{\cdot-}$) production in the yeast mitochondrial bc_1 complex, using decyl-ubiquinol as the electron donor, is 0.1-0.2 % of the electron transport rate (Table 1), a value similar to results in the literature obtained with bc_1 complex from yeast mitochondria [5, 7, 8, 44]. This is approximately the same rate, essentially a background rate, obtained in the presence of the p-side quinone analogue inhibitor DBMIB (Table 1), which prevents quinol oxidation by the [2Fe-2S] cluster [45]. Higher rates have been reported for mitochondrial bc_1 complexes, on the basis of difference in measurements with and without superoxide dismutase to assay $O_2^{\cdot-}$ production [44]. $O_2^{\cdot-}$ generation has also been measured with bc_1 complex obtained from the purple photosynthetic bacterium, *Rb. sphaeroides* [29, 46], for which the rate of $O_2^{\cdot-}$ production relative to the electron transport rate was not reported. In the present experiments with the yeast bc_1 complex, the specific rate of $O_2^{\cdot-}$ production, normalized to the electron transport rate, is, however, increased greatly (> 40-fold) in the presence of antimycin A (Table 1), in qualitative agreement with data obtained previously for the bc_1 complex [4, 5, 8, 27-29]. The electron transport rate of isolated b_6f complex or membranes from spinach and *M. laminosus*, and $O_2^{\cdot-}$ generation, was measured,

respectively, by the rate of reduction of plastocyanin, and by the rate of change of fluorescence emission intensity from the resorufin product of ADHP and H_2O_2 (*Materials and Methods*). Rates of electron transport (Fig. 3A) and $O_2^{\cdot-}$ production (Fig. 3B) obtained with yeast bc_1 complex and b_6f complex from spinach thylakoids and *M. laminosus* are shown, from which electron transport rates were derived for the yeast bc_1 complex (Table 1), purified b_6f complex isolated from spinach thylakoid membranes (Table 2), isolated *M. laminosus* cyanobacterial b_6f complex (Table 3), and membranes of *M. laminosus* (Table 4). The rate of $O_2^{\cdot-}$ production by electron transfer from the decyl-plastoquinol electron donor to b_6f complex (Table 2) is considerably higher, a factor of 10-20, than measured for the mitochondrial bc_1 complex (Table 1). Similar results were obtained with b_6f complex purified from the cyanobacterium, *M. laminosus*, using cyanobacterial plastocyanin (Table 3). Using intact membranes from *M. laminosus* (Table 4), the specific rate of superoxide production by the b_6f complex is larger that measured in isolated bc_1 complex by approximately an order of magnitude but, for reasons not understood, this rate is somewhat smaller that measured with isolated bc_1 complex (Table. 1).

Properties of inhibitors

(a) NQNO is an n-side quinone (Q_n) ligand of heme c_n [(1)], and it has been shown to inhibit oxidation of heme b_n [(32-34)]. NQNO binding to the b_6f complex in thylakoid membranes increases the amplitude of the flash-induced heme b_n reduction by a factor of 2-3 without significant inhibition of linear electron transport and oxygen evolution. In the present studies, concentrations of NQNO that affect the amplitude of heme b_n reduction only partly inhibit linear electron transport, and NQNO does not increase $O_2^{\cdot-}$ production as does addition of antimycin A to bc_1 complex (Tables 2-4 compared to Table 1). The difference in binding of n-side quinone analog inhibitors in the bc_1 and b_6f complexes resides in the multiple interactions with the amino acid environment that stabilize ligand-binding at the Q_n site of the bc_1 complex, whereas in the b_6f complex where heme c_n occludes access to heme b_n, the Q_n site protrudes into the inter-monomer cavity, with relatively few stabilizing interactions from coordinating amino acid residues. As a result, binding of a ligand such as NQNO at the Q_n-site is expected to be substantially weaker in the cytochrome b_6f complex than in the bc_1 complex. (**b**) DBMIB. Halogenated quinone analogs and in particular the dibromo-derivative DBMIB [(47)] have been described as potent inhibitors of the chloroplast cytochrome b_6f complex [(45)], and a less efficient inhibitor of the bc_1 complex from mitochondria [(48)]. DBMIB has been shown to bind at a position distal to the iron-sulfur binding site and also at this site [(45)]. In the present study, 2 μM DBMIB partially inhibits linear electron transport, and $O_2^{\cdot-}$ production of bc_1 complex to approximately 20% of the uninhibited rate (Table 1). Efficient inhibition is observed for cytochrome b_6f complex with rates of electron transport varying from undetectable to a few percent of the control (Tables 2-4), and no detectable $O_2^{\cdot-}$ production above the background signal.

Discussion

1. Origin of Elevated Superoxide Production in Cytochrome b_6f Complex

(A) More favorable redox potential of heme b_p in b_6f complex—(i) There is a large variation in the literature of midpoint redox potentials for heme b_p in the isolated

complex: (**i**) -90 mV, pH 7 [49]; (**ii**) -172 mV, pH 6.5 [50]; (**iii**) -80 mV, pH 6 [51]; -158 mV, pH 8.0 [52]. For the bc_1 complex, reported mid-point potentials of heme b_p are: approximately -30 mV in yeast and mammals [53, 54], -90/+50 mV in purple bacteria [55, 56], and 0 mV [57]. It is possible, but not determined by existing data, that a difference in redox potentials, e.g., a more negative potential of heme b_p in the b_6f complex, could contribute to the difference in efficiency of superoxide formation. However, the spread of data in the literature on the heme b_p redox potentials is presently too disparate to allow this explanation.

(B) Longer residence time—The higher rate of superoxide production in the b_6f compared to the bc_1 complex could arise from a longer residence time of the semiquinone in its binding niche ("Q_p pocket") proximal to the iron-sulfur cluster of the Rieske iron-sulfur protein. The 10-20 fold higher rate of $O_2^{\cdot-}$ production by the cytochrome b_6f complex compared to that of the bc_1 complex (Tables 2-4 vs. Table 1) implies that the rate constant in the b_6f complex for reactions (iib), (iii) or (v) above is increased relative to that for (**iv**). The source of this difference can be the $PQ_p^{\cdot-}$ generated in the b_6f complex having a longer life-time in the Q_p pocket relative to $UQ_p^{\cdot-}$ in the bc_1 complex. An identifiable structure-based cause of this longer residence time could be the partial occlusion of the Q_p-portal for quinone entry/exit by the phytyl chain of the unique chlorophyll-*a* molecule embedded in each monomer of the complex [31]. This occlusion does not affect the overall rate of electron transfer through the b_6f complex, as the isolated b_6f complex supports an electron transfer rate of ~200 electrons monomer^{-1} sec^{-1} at room temperature [58-60], which is comparable to the activity of the bc_1 complex measured in [61], and larger in the present experiments, than the activity of isolated bc_1 complex (Tables 2, 3 vs. Table 1). Therefore, quinol passage through the chlorophyll-obstructed portal is not the rate-limiting step in the photosynthetic linear electron transport chain.

(C) Role of the Glutamate in the Conserved PEWY Sequence in Semiquinone Formation—The neutral semiquinone species bound within the Q_p-site of cytochrome *bc* complexes undergoes deprotonation to form an anionic semiquinone (**formula** iii), which can be a proton donor to the low potential chain. It has been suggested that the Glu residue (Glu78 in subunit IV of cytochrome b_6f complex; Glu271 or Glu272 in the cytochrome *b* polypeptide in the bc_1 complex) of the conserved Pro-Glu-Trp-Tyr (PEWY) motif located on the p-side *ef*-loop is involved in deprotonation of the neutral semiquinone to the anionic semiquinone [62] (Fig. 4A, B), which acts as the electron donor to heme b_p (**formula** iib). Motion of the Glu271 residue in the cytochrome bc_1 complex during proton-transfer has been demonstrated [19, 63-66]. The Glu residue undergoes a rotation from a proton-extracting Q_p-niche proximal position, to a proton-releasing heme b_p-proximal position, where it interacts with the Tyr131 residue of cytochrome *b* (Fig. 4A). Hence, motion of the Glu residue constitutes an important step in the transfer of semiquinone from the Q_p-site. The kinetics of these reactions have recently been described [67].

In the cytochrome b_6f complex, electron density for the Glu78 residue side chain, homologous to the Glu271 residue in the bc_1 complex, was assigned recently in the 2.7 Å resolution crystal structure (PDB ID 4H44) [20]. The Glu78 residue side-chain is found in a heme b_p-proximal position, in which it interacts with a conserved Arg87 of the cytochrome

b_6 polypeptide through a short distance of 2.8 Å (Fig. 4B). In this position, the Glu78 side chain does not interact with the quinone analog inhibitor TDS (inserted into Q_p-site from PDB ID 4H13). The side chain of the conserved residue Tyr136 (cytochrome b_6 in the b_6f complex, trans-membrane helix C, Figs. 4B, C), which replaces Tyr131 of cytochrome *b* (bc_1 complex, Fig. 4A), does not interact with Glu78 in the heme b_p-proximal position. It has been previously reported that the conserved Arg87 of the trans-membrane helix B of the cytochrome b_6 polypeptide (b_6f complex, Fig. 4C) is replaced by a small uncharged residue, such as Ala84 (or Ala83), in cytochrome *b* (bc_1 complex, trans-membrane helix B) [68]. An analysis of the amino acid environment of Glu271 of cytochrome bc_1 shows that the Glu271 side chain is separated from the Ala84 residue by a distance of 7.3 Å (Fig. 4A). Hence, unlike the Glu78 residue in the b_6f complex that is inferred to participate in a relatively strong interaction with Arg87 in the heme b_p-proximal position, Glu271 in the bc_1 complex does not interact with a basic residue from the trans-membrane helix B in the heme b_p-proximal position. Thus, Glu271 may be relatively free to undergo motion in the cytochrome bc_1 complex, from a Q_p-niche proximal position to a heme b_p-proximal position, making proton extraction and translocation from the semiquinone a relatively efficient process. On the other hand, in the b_6f complex, motion of Glu78 is expected to be comparatively restricted due to the interaction with Arg87, thereby making proton translocation a less efficient process. As a consequence, the life-time of the neutral semiquinone is expected to be larger within the Q_p-site of the cytochrome b_6f complex.

2. Further consequences of increased semiquinone retention time

Photosynthetic state transitions depend on the redox poise of the thylakoid membrane quinone pool [69-71]. The presence of reduced plastoquinone in the Q_p-site activates a LHCII kinase bound to the b_6f complex [72, 73]. Regarding the application of this signaling process to cyanobacteria, although the latter possess state transitions that involve mobility of the phycobilisomes, this does not involve kinase activation, but is dependent on redox equilibria involving plastoquinone [11].

3. Chloroplasts as a major source of ROS in plant cells

High irradiance, and other stress conditions that affect photosynthetic electron transport rate and create hyperoxic conditions result in a transient increase in ROS in chloroplasts [9, 74]. The major sources of ROS generated in chloroplasts are PSII (singlet oxygen) and PSI ($O_2^{\cdot-}$). $O_2^{\cdot-}$ production by the cytochrome b_6f complex, as described in the present study, has been detected by EPR spectroscopy [12]. Accumulated $O_2^{\cdot-}$ can also be metabolized to another more stable form of ROS, hydrogen peroxide [11, 74].

The production of ROS in chloroplasts not only underlies oxidative damage inflicted during photosynthetic reactions [75], but the redox state of photosynthetic electron transport components conveys information about environmental light conditions. Thus, chloroplasts can function as mediators of environmental signals [76]. Light and stress induced generation of ROS contributes to redox signaling inside the chloroplast and from the organelle to the cytosol and nucleus [10, 77, 78]. ROS function in chloroplast signaling was demonstrated in relation to regulation dissipation and avoidance of excess excitation energy mechanisms [11]. The ROS generated in chloroplasts act as a retrograde signal to the nucleus for regulation of

plant responses to environmental stress and pathogen defense responses [79, 80]. Increases in H_2O_2 concentrations have been shown to be important for the induction of the ascorbate peroxidase gene, APX2, and for the expression of a number of genes involved in plant development and stress responses [81]. There is evidence that in plant disease resistance responses, ROS produced in chloroplasts interplay with signal from other intracellular and extracellular ROS sources in the modulation of pathogen-induced hypersensitive response [82, 83].

Acknowledgments

We thank Prof. B. L. Trumpower for providing yeast bc_1 complex and for helpful discussions.

Funding: These studies were supported by NIH grant R01-GM038323, the Henry Koffler Distinguished Professorship (WAC), a Purdue University Fellowship (SSH), and infra-structure support from the Purdue University Cancer Center.

References

1. Yamashita E, Zhang H, Cramer WA. Structure of the cytochrome b_6f complex: quinone analogue inhibitors as ligands of heme c_n. J Mol Biol. 2007; 370:39–52. [PubMed: 17498743]
2. Cape JL, Bowman MK, Kramer DM. Understanding the cytochrome *bc* complexes by what they don't do, The Q-cycle at 30. Trends Plant Sci. 2006; 11:46–55. [PubMed: 16352458]
3. Cape JL, Bowman MK, Kramer DM. A semiquinone intermediate generated at the Q_o site of the cytochrome bc_1 complex: importance for the Q-cycle and superoxide production. Proc Natl Acad Sci, USA. 2007; 104:7887–7892. [PubMed: 17470780]
4. Drose S, Brandt U. The mechanism of mitochondrial superoxide production by the cytochrome bc_1 complex. J Biol Chem. 2008; 283:21649–21654. [PubMed: 18522938]
5. Forquer I, Covian R, Bowman MK, Trumpower B, Kramer DM. Similar transition states mediate the Q-cycle and superoxide production by the cytochrome bc_1 complex. J Biol Chem. 2006; 281:38459–38465. [PubMed: 17008316]
6. Lanciano P, Khalfaoui-Hassani B, Selamoglu N, Ghelli A, Rugolo M, Daldal F. Molecular mechanisms of superoxide production by complex III: a bacterial versus human mitochondrial comparative case study. Biochim Biophys Acta. 2013; 1827:1332–1339. [PubMed: 23542447]
7. Muller F, Crofts AR, Kramer DM. Multiple Q-cycle bypass reactions at the Q_o site of the cytochrome bc_1 complex. Biochemistry. 2002; 41:7866–7874. [PubMed: 12069575]
8. Muller FL, Roberts AG, Bowman MK, Kramer DM. Architecture of the Q_o site of the cytochrome bc_1 complex probed by superoxide production. Biochemistry. 2003; 42:6493–6499. [PubMed: 12767232]
9. Mittler R, Vanderauwera S, Gollery M, Van Breusegem F. Reactive oxygen gene network of plants. Trends Plant Sci. 2004; 9:490–498. [PubMed: 15465684]
10. Mittler R, Vanderauwera S, Suzuki N, Miller G, Tognetti VB, Vandepoele K, Gollery M, Shulaev V, Van Breusegem F. ROS signaling: The new wave? Trends Plant Sci. 2011; 16:300–309. [PubMed: 21482172]
11. Mullineaux P, Karpinski S. Signal transduction in response to excess light: Getting out of the chloroplast. Curr Opin Plant Biol. 2002; 5:43–48. [PubMed: 11788307]
12. Sang M, Xie J, Qin XC, Wang WD, Chen XB, Wang KB, Zhang JP, Li LB, Kuang TY. High-light induced superoxide radical formation in cytochrome b_6f complex from *Bryopsis corticulans* as detected by EPR spectroscopy. J Photochem Photobiol B. 2011; 102:177–181. [PubMed: 21277495]
13. Petlicki J, Van de Ven TGM. The equilibrium between the oxidation of hydrogen peroxide by oxygen and the dismutation of peroxyl or superoxide radicals in aqueous solutions in contact with oxygen. J Chem Soc, Fara Trans. 1998; 94:2763–2767.

14. Wood PM. The potential diagram for oxygen at pH 7. Biochem J. 1988; 253:287–289. [PubMed: 2844170]
15. Trumpower BL, Gennis RB. Energy transduction by cytochrome complexes in mitochondrial and bacterial respiration:the enzymology of coupling electron transfer reactions to transmembrane proton translocation. Ann Rev Biochem. 1994; 63:675–716. [PubMed: 7979252]
16. Cramer WA, Yamashita E, Hasan SS. The Q cycle of cytochrome bc complexes: A structure perspective. Biochim Biophys Acta-Bioenergetics. 2011; 1807:788–802.
17. Okayama S. Redox potential of plastoquinone A in spinach chloroplasts. Biochim Biophys Acta. 1976; 440:331–336. [PubMed: 8122]
18. Trumpower BL. The protonmotive Q cycle Energy transduction by coupling of proton translocation to electron transfer by the cytochrome bc_1 complex. J Biol Chem. 1990; 265:11409–11412. [PubMed: 2164001]
19. Crofts AR, Hong S, Ugulava N, Barquera B, Gennis R, Guergova-Kuras M, Berry EA. Pathways for proton release during ubihydroquinone oxidation by the bc_1 complex. Proc Natl Acad Sci, USA. 1999; 96:10021–10026. [PubMed: 10468555]
20. Hasan SS, Yamashita E, Baniulis D, Cramer WA. Quinone-dependent proton transfer pathways in the photosynthetic cytochrome b_6f complex. Proc Natl Acad Sci, USA. 2013; 110:4297–4302. [PubMed: 23440205]
21. Berry EA, Guergova-Kuras M, Huang LS, Crofts AR. Structure and function of cytochrome *bc* complexes. Ann Rev Biochem. 2000; 69:1005–1075. [PubMed: 10966481]
22. Crofts AR. The cytochrome bc_1 complex: function in the context of structure. Annu Rev Physiol. 2004; 66:689–733. [PubMed: 14977419]
23. Mitchell P. The protonmotive Q cycle: A general formulation. FEBS Lett. 1975; 59:137–139. [PubMed: 1227927]
24. Joliot P, Joliot A. The low-potential electron-transfer chain in the cytochrome *bf* complex. Biochim Biophys Acta. 1988; 933:319–333.
25. Sarewicz M, Borek A, Cieluch E, Swierczek M, Osyczka A. Discrimination between two possible reaction sequences that create potential risk of generation of deleterious radicals by cytochrome bc_1. Implications for the mechanism of superoxide production. Biochim Biophys Acta. 2010; 1797:1820–1827. [PubMed: 20637719]
26. Huang LS, Cobessi D, Tung EY, Berry EA. Binding of the respiratory chain inhibitor antimycin to the mitochondrial bc_1 complex: a new crystal structure reveals an altered intramolecular hydrogen-bonding pattern. J Mol Biol. 2005; 351:573–597. [PubMed: 16024040]
27. Berry EA, Huang LS, Lee DW, Daldal F, Nagai K, Minagawa N. Ascochlorin is a novel, specific inhibitor of the mitochondrial cytochrome bc_1complex. Biochim Biophys Acta. 2010; 1797:360–370. [PubMed: 20025846]
28. Rottenberg H, Covian R, Trumpower BL. Membrane potential greatly enhances superoxide generation by the cytochrome bc_1 complex reconstituted into phospholipid vesicles. J Biol Chem. 2009; 284:19203–19210. [PubMed: 19478336]
29. Yin Y, Tso SC, Yu CA, Yu L. Effect of subunit IV on superoxide generation by *Rhodobacter sphaeroides* cytochrome bc_1 complex. Biochim Biophys Acta. 2009; 1787:913–919. [PubMed: 19348783]
30. Kurisu G, Zhang H, Smith JL, Cramer WA. Structure of the cytochrome b_6f complex of oxygenic photosynthesis: Tuning the cavity. Science. 2003; 302:1009–1014. [PubMed: 14526088]
31. Hasan SS, Yamashita E, Cramer WA. Trans-membrane signaling and assembly of the cytochrome b_6f-lipidic charge transfer complex. Biochim Biophys Acta. 2013; 1827:1295–1308. [PubMed: 23507619]
32. Jones RW, Whitmarsh J. Inhibition of electron transfer and electrogenic reaction in the cytochrome *b/f* complex by 2-n-nonyl-4-hydroxyquinoline N-oxide (NQNO) and 2,5-dibromo-3methyl-6-isopropyl-p-benzoquinone (DBMIB). Biochim Biophys Acta. 1988; 933:258–268.
33. Rich PR, Madgwick SA, Moss DA. The interactions of duroquinol, DBMIB, and NQNO with the chloroplast cytochrome *bf* complex. Biochim Biophys Acta. 1991; 1058:312–328.
34. Furbacher PN, Girvin ME, Cramer WA. On the question of interheme electron transfer in the chloroplast cytochrome b_6 *in situ*. Biochemistry. 1989; 28:8990–8998. [PubMed: 2605237]

35. Baniulis, D.; Zhang, H.; Yamashita, E.; Zakharova, T.; Hasan, SS.; Cramer, WA. Purification and crystallization of the cyanobacterial cytochrome b_6f complex. In: Carpentier, R., editor. Methods Mol Biol (Photosyn Res Protoc). Humana Press Inc; Totowa, NJ: 2011. p. 65-77.
36. Cramer, WA.; Yamashita, E.; Baniulis, D.; Hasan, SS. The cytochrome b_6f complex of oxygenic photosynthesis. In: Messerschmidt, A., editor. Handbook of Metalloproteins. John Wiley & Sons; Chichester: 2011. p. 16-28.
37. Morand LZ, Krogmann DW. Large scale preparation of pure plastocyanin from spinach. Biochim Biophy Acta. 1993; 1141:105–106.
38. Massey V. The microestimation of succinate and the extinction coefficient of cytochrome *c*. Biochim Biophys Acta. 1959; 34:255–256. [PubMed: 14422133]
39. Christensen HEM. A new procedure for the fast isolation and purification of plastocyanin from the cyanobacterium. A variabilis Photosyn Res. 1990; 25:72–76.
40. Sievers F, Wilm A, Dineen DD, Gibson TJ, Karplus K, Li W, Lopez R, McWilliam H, Remmert M, Soeding J, Thompson JD, Higgins DG. Fast scalable generation of high-quality protein multiple seqiuence alignments using Clustal Omega. Mol Sys Biol. 2011; 7:539.
41. Goujon M, McWilliam H, Li W, Valentin F, Squizzato S, Paern J, Lopez R. A new bioinformatics analysis tools framework at EMBL-EBI. Nucleic Acids Res. 2010; 38:W695–699. [PubMed: 20439314]
42. Gao X, Wen X, Esser L, Quinn B, Yu L, Yu CA, Xia D. Structural basis for the quinone reduction in the bc_1 complex: A comparative analysis of crystal structures of mitochondrial cytochrome bc_1 with bound substrate and inhibitors at the Q_i site. Biochemistry. 2003; 42:9067–9080. [PubMed: 12885240]
43. Solmaz SR, Hunte C. Structure of complex III with bound cytochrome c in reduced state and definition of a minimal core interface for electron transfer. J Biol Chem. 2008; 283:17542–17549. [PubMed: 18390544]
44. Sun J, Trumpower BL. Superoxide anion generation by the cytochrome bc_1 complex. Arch Biochem Biophys. 2003; 419:198–206. [PubMed: 14592463]
45. Yan J, Kurisu G, Cramer WA. Intraprotein transfer of the quinone analogue inhibitor 2,5-dibromo-3-methyl-6-isopropyl-p-benzoquinone in the cytochrome b_6f complex. Proc Natl Acad Sci, USA. 2006; 103:69–74. [PubMed: 16371475]
46. Yin Y, Yang S, Yu L, Yu CA. Reaction mechanism of superoxide generation during ubiquinol oxidation by the cytochrome bc_1 complex. J Biol Chem. 2010; 285:17038–17045. [PubMed: 20371599]
47. Bohme H, Reimer S, Trebst A. Role of plastoquinone in photosynthesis - Effect of dibromothymoquinone, an antagonist of plastoquinone, on non cyclic and cyclic electron flow systems in isolated chloroplasts. Z Naturforsc B. 1971; 26:341–352.
48. Gwak SH, Yang FD, Yu L, Yu CA. Phospholipid-dependent interaction between dithymoquinone and iron-sulfur protein in mitochondrial cytochrome *c* reductase. Biochim Biophys Acta. 1987; 890:319–325. [PubMed: 3028477]
49. Rich PR, Bendall DS. The redox potentials for the *b*-type cytochromes of higher plant chloroplasts. Biochim Biophys Acta. 1980; 591:153–161. [PubMed: 7388012]
50. Hurt E, Hauska G. Identification of the polypeptides in the cytochrome b_6f complex from spinach chloroplasts with redox-center-carrying subunits. J Bioenerg Biomemb. 1982; 14:405–424.
51. Hurt EC, Hauska G. Cytochrome b_6 from isolated cytochrome b_6f complexes - evidence for two spectral forms with different midpoint potentials. FEBS Lett. 1983; 153:413–419.
52. Pierre Y, Breyton C, Kramer D, Popot JL. Purification and characterization of the cytochrome b_6f complex from *Chlamydomonas reinhardtii*. J Biol Chem. 1995; 270:29342–29349. [PubMed: 7493968]
53. Wikström MKF. The different cytochrome *b* components in the respiratory chain of animal mitochondria and their role in electron transport and energy conservation. Biochim Biophys Acta. 1973; 301:155–193. [PubMed: 4358869]
54. T'Sai AL, Palmer G. Potentiometric studies on yeast complex III. Biochim Biophys Acta. 1983; 722:349–363. [PubMed: 6301554]

55. Dutton PL, Jackson JB. Thermodynamic and kinetic characterization of electron transfer components *in situ* in *Rhodopseudomonas spheroides* and *Rhodospirillum rubrum*. Eur J Biochem. 1972; 30:495–510. [PubMed: 4344828]
56. Crofts AR, Meinhardt SW, Jones KR, Snozzi M. The Role of the Quinone Pool in the Cyclic Electron-Transfer Chain on *Rhodopseudomonas sphaeroides* - a Modified Q-Cycle Mechanism. Biochim Biophys Acta. 1983; 723:202–218. [PubMed: 21494412]
57. Yun CH, Crofts AR, Gennis RB. Assignment of the histidine axial ligands to the cytochrome bH and cytochrome bL components of the bc_1 complex from *Rhodobacter sphaeroides* by site-directed mutagenesis. Biochemistry. 1991; 30:6747–6754. [PubMed: 1648391]
58. Baniulis D, Yamashita E, Whitelegge JP, Zatsman AI, Hendrich MP, Hasan SS, Ryan CM, Cramer WA. Structure-function, stability, and chemical modification of the cyanobacterial cytochrome b_6f complex from *Nostoc* sp. PCC 7120. J Biol Chem. 2009; 284:9861–9869. [PubMed: 19189962]
59. Zhang H, Kurisu G, Smith JL, Cramer WA. A defined protein-detergent-lipid complex for crystallization of integral membrane proteins: The cytochrome b_6f complex of oxygenic photosynthesis. Proc Nat Acad Sci USA. 2003; 100:5160–5163. [PubMed: 12702760]
60. Zhang H, Whitelegge JP, Cramer WA. Ferredoxin:$NADP^+$ oxidoreductase is a subunit of the chloroplast cytochrome b_6f complex. J Biol Chem. 2001; 276:38159–38165. [PubMed: 11483610]
61. Yu L, Yang S, Yin Y, Cen X, Zhou F, Xia D, Yu CA. Analysis of electron transfer and superoxide generation in the cytochrome bc_1 complex. Methods Enzymol. 2009; 456:459–473. [PubMed: 19348904]
62. Zito F, Finazzi G, Joliot P, Wollman FA. Glu78, from the conserved PEWY sequence of subunit IV, has a key function in cytochrome b_6f turnover. Biochemistry. 1998; 37:10395–10403. [PubMed: 9671508]
63. Crofts AR, Barquera B, Gennis RB, Kuras R, Guergova-Kuras M, Berry EA. Mechanism of ubiquinol oxidation by the bc_1 complex: different domains of the quinol binding pocket and their role in the mechanism and binding of inhibitors. Biochemistry. 1999; 38:15807–15826. [PubMed: 10625446]
64. Hunte C, Koepke J, Lange C, Rossmanith T, Michel H. Structure at 2.3 Å resolution of the cytochrome bc_1 complex from the yeast *Saccharomyces cerevisiae* co-crystallized with an antibody Fv fragment. Structure. 2000; 8:669–684. [PubMed: 10873857]
65. Palsdottir H, Lojero CG, Trumpower BL, Hunte C. Structure of the yeast cytochrome bc_1 complex with a hydroxyquinone anion Q_o site inhibitor bound. J Biol Chem. 2003; 278:31303–31311. [PubMed: 12782631]
66. Izrailev S, Crofts AR, Berry EA, Schulten K. Steered molecular dynamics simulation of the Rieske subunit motion in the cytochrome bc_1 complex. Biophys J. 1999; 77:1753–1768. [PubMed: 10512801]
67. Victoria D, Burton R, Crofts AR. Role of the -PEWY-glutamate in catalysis at the Q_o-site of the Cyt bc_1 complex. Biochim Biophys Acta. 2013; 1827:365–386. [PubMed: 23123515]
68. Widger WR, Cramer WA, Herrmann RG, Trebst A. Sequence homology and structural similarity between the *b* cytochrome of mitochondrial complex III and the chloroplast b_6f complex: position of the cytochrome *b* hemes in the membrane. Proc Natl Acad Sci, USA. 1984; 81:674–678. [PubMed: 6322162]
69. Allen JF, Bennett J, Steinback KE, Arntzen CJ. Chloroplast Protein-Phosphorylation Couples Plastoquinone Redox State to Distribution of Excitation-Energy between Photosystems. Nature. 1981; 291:25–29.
70. Allen JF, Horton P. Chloroplast Protein-Phosphorylation and Chlorophyll Fluorescence Quenching-Activation by Tetramethyl-Para-Hydroquinone, an Electron-Donor to Plastoquinone. Biochim Biophys Acta. 1981; 638:290–295.
71. Horton P, Allen JF, Black MT, Bennett J. Regulation of Phosphorylation of Chloroplast Membrane Polypeptides by the Redox State of Plastoquinone. FEBS Lett. 1981; 125:193–196.
72. Lemeille S, Willig A, Depege-Fargeix N, Delessert C, Bassi R, Rochaix JD. Analysis of the chloroplast protein kinase Stt7 during state transitions. PLoS Biol. 2009; 7:664–675.
73. Rochaix JD. Regulation of photosynthetic electron transport. Biochim Biophys Acta. 2011; 1807:375–383. [PubMed: 21118674]

74. Apel K, Hirt H. Reactive oxygen species: Metabolism, oxidative stress, and signal transduction. Ann Rev Plant Biol. 2004; 55:373–399. [PubMed: 15377225]

75. Foyer CH, Shigeoka S. Understanding oxidative stress and antioxidant functions to enhance photosynthesis. Plant Physiol. 2011; 155:93–100. [PubMed: 21045124]

76. Pfannschmidt T, Schutze K, Brost M, Oelmuller R. A novel mechanism of nuclear photosynthesis gene regulation by redox signals from the chloroplast during photosystem stoichiometry adjustment. J Biol Chem. 2001; 276:36125–36130. [PubMed: 11468291]

77. Fernandez AP, Strand A. Retrograde signalling and plant stress: plastid signals initiate cellular stress responses. Curr Opin Plant Biol. 2008; 11:509–513. [PubMed: 18639482]

78. Strand, A.; Kleine, T.; Chory, T. Struc Func Plastids Adv Photosyn Resp. Springer; 2007. Plastid-to-nucleus signaling; p. 183-197.

79. Inaba T, Yazu F, Ito-Inaba Y, Kakizaki T, Nakayama K. Retrograde signaling pathway from plastid to nucleus. Intern Rev Cell Mol Biol. 2011; 290:167–204.

80. de Dios Barajas-Lopez J, Blanco NE, Strand A. Plastid-to-nucleus communication, signals controlling the running of the plant cell. Biochim Biophys Acta. 2013; 1833:425–437. [PubMed: 22749883]

81. Vanderauwera S, Zimmermann P, Rombauts S, Vandenabeele S, Langebartels C, Gruissem W, Inze D, Van Breusegem F. Genome-wide analysis of hydrogen peroxide-regulated gene expression in *Arabidopsis* reveals a high light-induced transcriptional cluster involved in anthocyanin biosynthesis. Plant Physiol. 2005; 139:806–821. [PubMed: 16183842]

82. Kangasjarvi S, Neukermans J, Li S, Aro EM, Noctor G. Photosynthesis, photorespiration, and light signalling in defence responses. J Exp Bot. 2012; 63:1619–1636. [PubMed: 22282535]

83. Zurbriggen MD, Carrillo N, Hajirezaei MR. ROS signaling in the hypersensitive response. When, where and what for? Plant Signal Behav. 2011; 5:393–396. [PubMed: 20383072]

Abbreviations

ADPH	10-acetyl-3,7-dihydroxyphenoxazine
b_p and b_n	*b*-hemes on electrochemically positive and negative sides of b_6f complex
Chl-*a*	chlorophyll
DBMIB	2,5-dibromo-3-methyl-6-isopropyl-*p*-benzoquinone
DDM, UDM	n-dodecyl- or undecyl-β-D-maltopyranoside
$\Delta\tilde{\mu}_h^+$	trans-membrane proton electrochemical potential gradient
E_{m7}	midpoint oxidation-reduction potential at pH 7
ISP	iron-sulfur protein
HRP	horseradish peroxidase
MOPS	3-(N-morpholino) propanesulfonic acid
NQNO	2-n-nonyl-4-hydroxyquinoline-N-oxide
p, n	electrochemically positive, negative side of membrane and cytochrome *bc* complexes
PC	plastocyanin
PSI	II, photosystem I, II
Q	quinone

Q_p	p-side quinone binding site
PQ/PQH_2	plastoquinone/-ol
$PQ_p^{\cdot-}$	plastosemiquinone
ROS	reactive oxygen species
$O_2^{\cdot-}$	superoxide
SOD	superoxide dismutase
STG	stigmatellin
TDS	tridecyl-stigmatellin
UQ/UQH_2	ubiquinone/-ol
$UQ^{\cdot-}$	ubisemiquinone

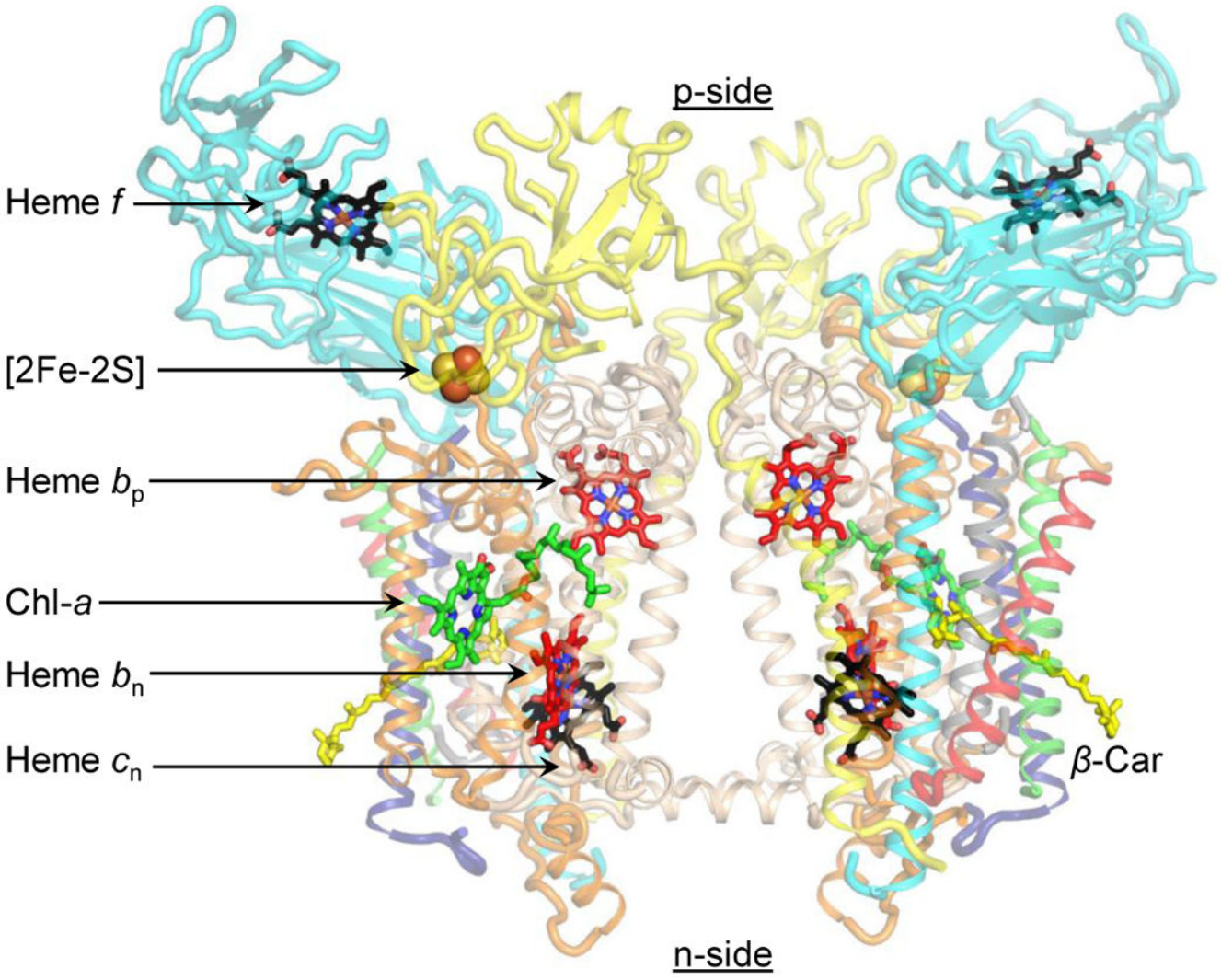

Figure 1.

The dimeric cytochrome b_6f complex (PDB ID 4H44). Prosthetic groups in the cytochrome b_6f complex. Hemes b_p (red), b_n (red) and c_n (black) are redox-active prosthetic groups located within the trans-membrane domain, and constitute the low-potential chain. Heme *f* (black) and [2Fe-2S] cluster (orange/yellow spheres) form the high-potential chain, and are associated with the p-side extrinsic domains of cytochrome *f* and ISP, respectively. A chlorophyll-*a* (green) and a *β*-carotene (yellow) are also associated with the complex. Polypeptides are shown as ribbons. Color code: cytochrome b_6 (cyt b_6), wheat; subunit IV (subIV), orange; cytochrome *f* (cyt *f*), cyan; iron-sulfur protein (ISP), yellow; PetL, red; PetM, green; PetG, blue; PetN, gray.

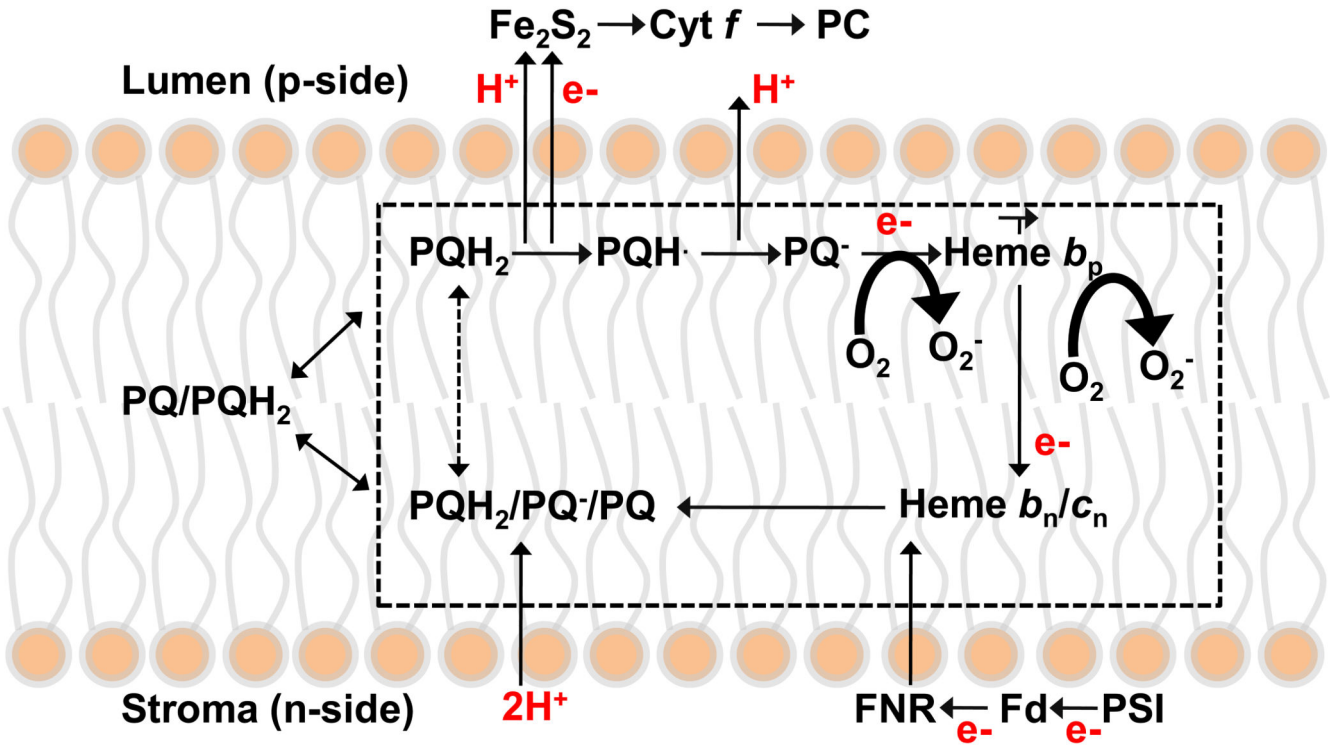

Figure 2.

Trans-membrane electron transfer and *Q*-cycle mechanism in a schematic of the cytochrome b_6f complex, indicating the branching of electrons from the anionic semiquinone reductant, $PQ_p^{\cdot-}$ and heme b_p to O_2, the latter reactions responsible for formation of superoxide, $O_2^{\cdot-}$.

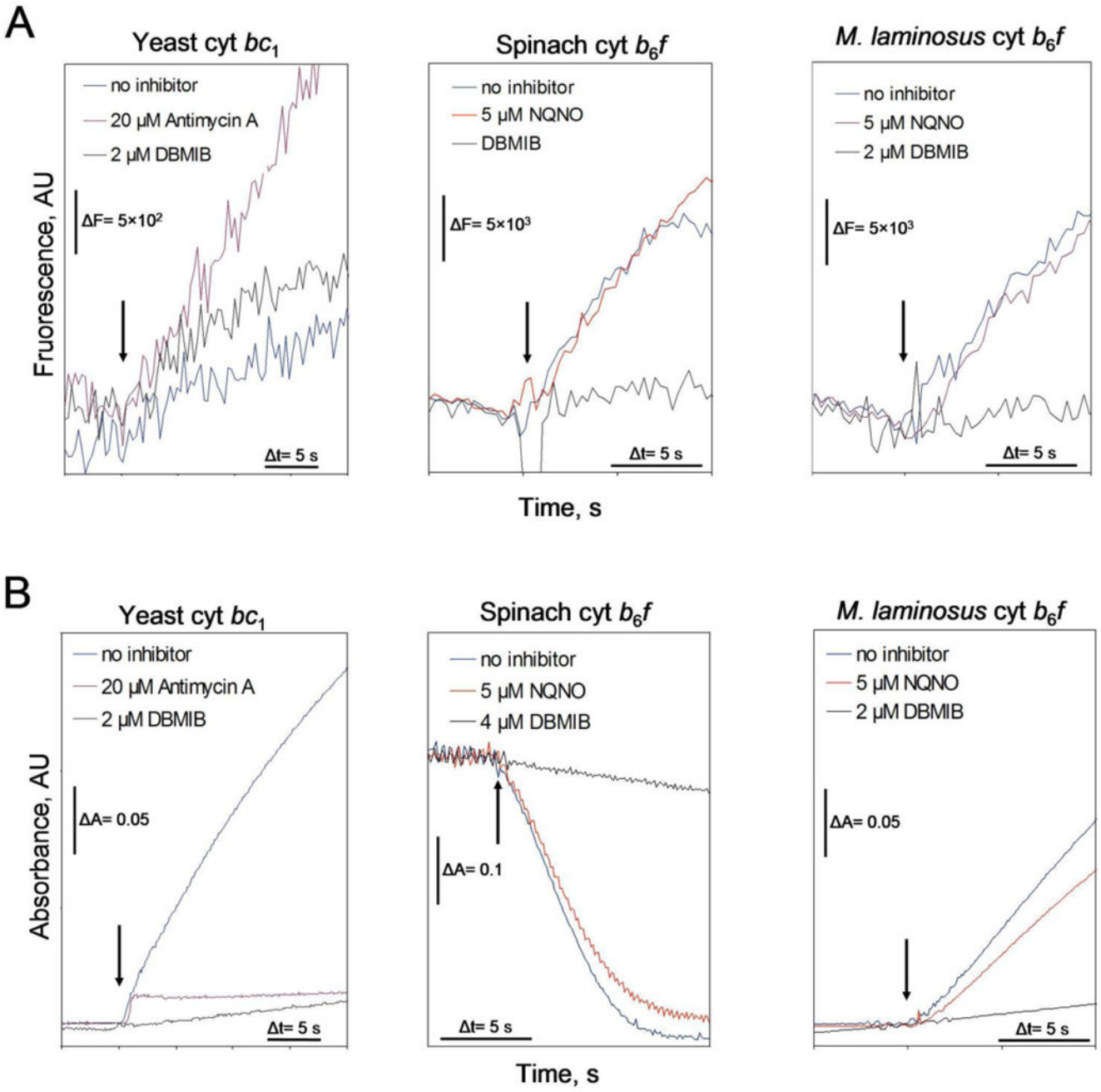

Figure 3.

Representative original data traces for determination of rates of (**A, upper traces**) superoxide generation and (**B, lower traces**) electron transfer in isolated bc_1 and b_6f complexes. The electron transfer and superoxide generation activities were measured as described in **Materials and Methods** using cytochrome *c* as the electron acceptor for the yeast cyt bc_1, cyt b_6f from *M. laminosus*, and cyanobacterial plastocyanin for the b_6f complex from spinach. Traces averaged from two to four measurements are shown. The background fluorescence change measured for the reaction mixture before the addition of the enzyme was subtracted from the superoxide generation activity data (**B, lower traces**).

The arrow indicates addition of 5 nM and 45 nM bc_1 complex, respectively, for reactions in the absence and presence of inhibitor, and 5 nM b_6f complex.

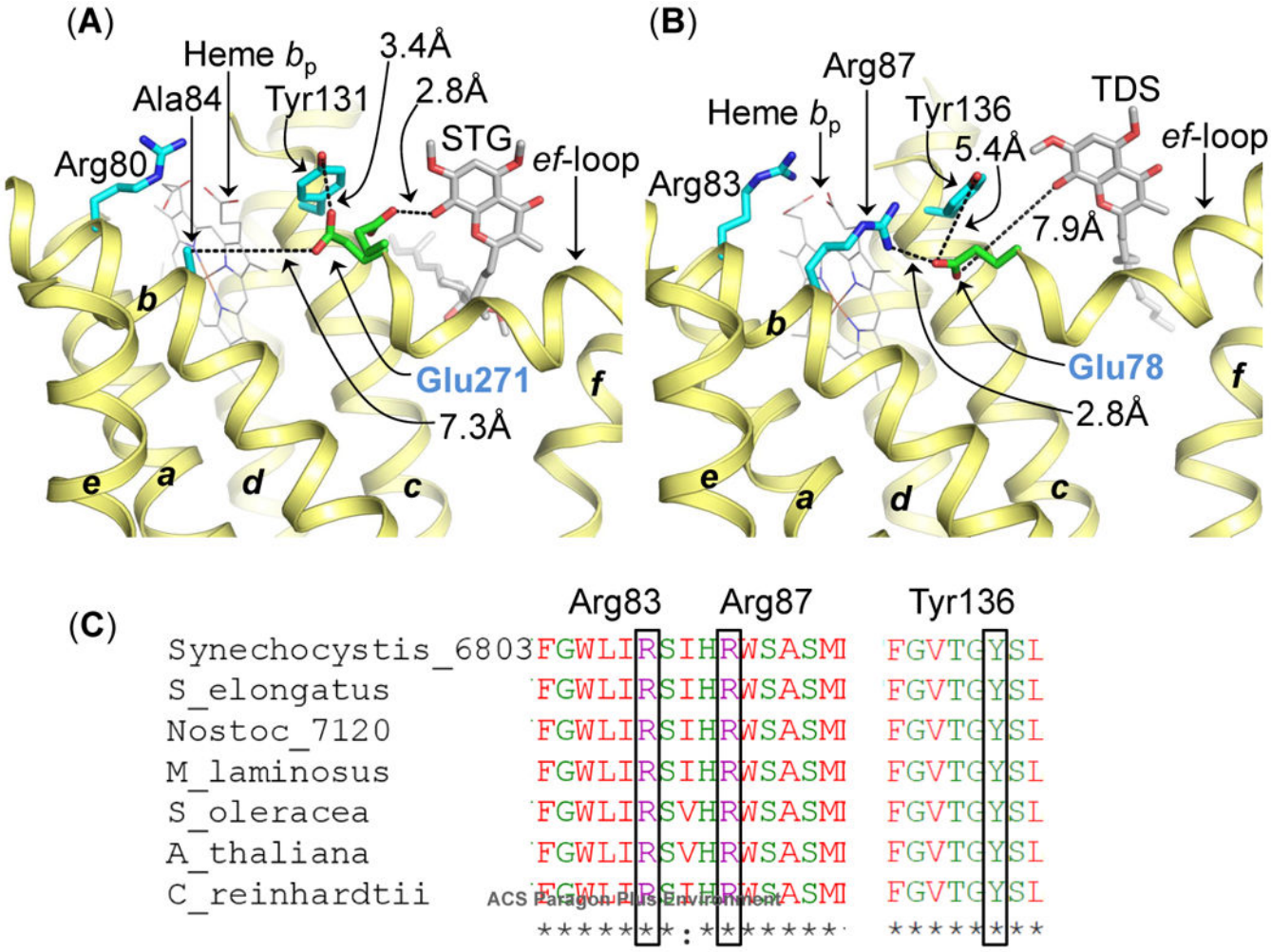

Figure 4.

Role of conserved Glu (Pro-Glu-Trp-Tyr) in semiquinone deprotonation in cyochrome *bc* complexes. (**A**) In the bc_1 complex, the Glu271 residue (green/red stcks, labeled in blue) of the PEWY sequence is found to occupy two distinct locations-quinone proximal (PDB ID 3CX5) and heme b_p-proximal (PDB ID 1NTZ). In the heme b_p-proximal position, Glu271 inteacts with Tyr131 (cytochrome *b* polypeptide). The figure was generated by superposition of cytochrome bc_1 crystal structures (PDB IDs 1NTZ and 3CX5). The STG molecule and the quinone/STG-proximal Glu271 orientation were obtained from PDB ID 3CX5. (**B**) In the cytochrome b_6f complex crystal structure (PDB ID 4H44), Glu78 (green/red sticks, labeled in blue) of subunitIV, homologous to Glu271 in the bc_1 complex, is located in the heme b_p-proximal orientation. In this position, Glu78 interacts with Arg87 of cytochrome b_6 (b_6f), through a distance of 2.8 Å. Arg87 (b_6f) is replaced by Ala84 (cyan sticks) in the bc_1 complex. Arg83 of cytochrome b_6 (b_6f) and Arg80 of cytochrome *b* (bc_1) are conserved in their location. The quinone analog inhibitor TDS has been inserted into the figure from PDB ID 4H13 to mark the Q_p-site. The transmembrane helices (*a*-*g*) are labeled. The polypeptides are shown as ribbons. (**C**) Multiple sequence alignment of the cytochrome b_6 subunit of the cytochrome b_6f complex from prokaryotic cyanobacteria (*Synechocystis* PCC 6803,

Synechococcus elongates PCC 6301, *Nostoc* PCC 7120, *M. laminosus*), a eukaryotic alga (*C. reinhardtii*), and higher plants (*Arabidopsis thaliana* and *Spinacea oleracea*). Arg83, Arg87 (trans-membrane helix B) and Tyr136 (trans-membrane helix C) are conserved in cytochrome b_6 polypeptide.

Table 1

Superoxide Production by Cytochrome bc_1 Complex from Yeast Mitochondria

	Electron transfer rate, Cyt $bc^{-1} \cdot s^{-1}$	Superoxide production rate Cyt $bc_1^{-1} \cdot s^{-1}$	Superoxide production (% electron transfer rate)
Control, no inhibitor [1]	151 ± 6.1 (n=5)	0.21 ± 0.13 (n=8)	0.14 ± 0.06
Antimycin A, 20 μM	1.2 ± 0.1 (n=4)	0.13 ± 0.03 (n=6)	10.6 ± 2.3
DBMIB, 2 μM	28.3 ± 3.1 (n=4)	0.04 ± 0.01 (n=3)	0.14 ± 0.02

[1] for reactions in the absence and presence of inhibitor, bc_1 complex was used at 5 nM and 45 nM, respectively, with cytochrome *c* as electron acceptor; n, number of trials.

Table 2

Superoxide Production by Isolated Spinach Cytochrome b_6f Complex; Electron Acceptor, Plastocyanin

	Electron transfer rate, Cyt $b_6f^{-1} \cdot s^{-1}$	Superoxide production rate Cyt $b_6f^{-1} \cdot s^{-1}$	Superoxide production (% electron transfer rate)
Control, no inhibitor	245 ± 25 (n=10)	4.5 ± 0.6 (n=10)	1.9 ± 0.3
NQNO, 5 μM	196 ± 7 (n=3)	3.5 ± 0.4 (n=3)	1.8 ± 0.2
DBMIB, 4 μM	n.d. (n=4)	n.d. (n=3)	-

n, number of trials; n.d., rate too small to allow accurate determination.

Table 3

Superoxide Production by Isolated Cytochrome b_6f Complex from the Cyanobacterium, *M. laminosus*; Electron Acceptor, Cyanobacterial Plastocyanin

	Electron transfer rate, Cyt $b_6f^{-1} \cdot s^{-1}$	Superoxide production rate, Cyt $b_6f^{-1} \cdot s^{-1}$	Superoxide production rate (% electron transfer rate)
Control, no inhibitor	292 (n=2)	6.3 (n=2)	2.2 (n=2)
NQNO, 5 μM	174 (n=1)	2.3 (n=1)	2.2 (n=1)
DBMIB, 2 μM	6.5 ± 1.0 (n=3)	n.d. (n=6)	-
DBMIB, 5 μM	0.5 ± 0.7 (n=3)	n.d. (n=4)	-

n, number of trials; n .d., not determined.

Table 4

Superoxide Production by Cytochrome b_6f Complex in Thylakoid Membranes from the Cyanobacterium, *M. laminosus*; Electron Acceptor, Cytochrome *c*

	Electron transfer rate, 10^3 chl $a^{-1} \cdot s^{-1}$	Superoxide production rate 10^3 chl $a^{-1} \cdot s^{-1}$	Superoxide production rate (% electron transfer rate)
Control, no inhibitor	201 ± 3 (n=3)	2.6 ± 0.6 (n=4)	1.3 ± 0.3
NQNO, 5 μM	151 ± 8 (n=3)	1.5 ± 0.1 (n=3)	0.9 ± 0.1
DBMIB, 2 μM	11 ± 2 (n=3)	n.d. (n=3)	-
DBMIB, 5 μM	0.2 ± 0.4 (n=3)	n.d. (n=3)	-

n, number of trials; n .d., not determined.